

Determination of earthquake safety of RC frame structures using an energy-based approach

Onur Merter^{1a}, Taner Ucar^{*2} and Mustafa Duzgun^{1b}

¹Department of Civil Engineering, Dokuz Eylul University, 35160, Buca, Izmir, Turkey

²Department of Architecture, Dokuz Eylul University, 35160, Buca, Izmir, Turkey

(Received January 6, 2016, Revised February 17, 2017, Accepted February 25, 2017)

Abstract. An energy-based approach for determining earthquake safety of reinforced concrete frame structures is presented. The developed approach is based on comparison of plastic energy capacities of the structures with plastic energy demands obtained for selected earthquake records. Plastic energy capacities of the selected reinforced concrete frames are determined graphically by analyzing plastic hinge regions with the developed equations. Seven earthquake records are chosen to perform the nonlinear time history analyses. Earthquake plastic energy demands are determined from nonlinear time history analyses and hysteretic behavior of earthquakes is converted to monotonic behavior by using nonlinear moment-rotation relations of plastic hinges and plastic axial deformations in columns. Earthquake safety of selected reinforced concrete frames is assessed by using plastic energy capacity graphs and earthquake plastic energy demands. The plastic energy dissipation capacities of the frame structures are examined whether these capacities can withstand the plastic energy demands for selected earthquakes or not. The displacements correspond to the mean plastic energy demands are obtained quite close to the displacements determined by using the procedures given in different seismic design codes.

Keywords: energy-based approach; earthquake safety; reinforced concrete frames; nonlinear static pushover analysis; plastic energy; nonlinear time history analysis

1. Introduction

Determination of earthquake safety of structures is the most popular and important one among the topics of structural and earthquake engineering. Displacement and energy based many different analysis methods, both static and dynamic, can be used in determination of earthquake safety of structures. In nonlinear dynamic analysis methods, different nonlinear response quantities might be obtained by using recorded or artificial earthquake time histories. Although dynamic analysis methods are assumed to be more realistic, these kinds of analysis methods are impractical due to its conceptual and numerical sophistication, complexity in modeling the cyclic force-deformation relations of reinforced concrete (RC) sections, scaling of earthquakes and the huge amount of time required. Therefore, nonlinear static analysis methods, which are more practical, have become widely used analytical tools in earthquake safety analysis of structures.

In displacement-based analysis methods, which are the most widely used in determination of earthquake safety of structures, force-deformation capacities of structures are

determined by nonlinear static analyses, or so-called pushover analyses. In single mode and multi-mode pushover analyses, the structure is incrementally pushed with monotonously increasing amplitude of lateral loads and the capacity of the structure is represented by a nonlinear lateral load-displacement curve, which is referred to as a capacity curve. The estimated strength and deformation demands of an earthquake ground motion excitation or design earthquake on the structure are determined and the expected performance of the structure is evaluated by comparing these demands to capacities specified at different codes. In these methods, the target displacement is typically controlled at the roof level of the structure. The most current nonlinear static procedures use lateral load patterns based on the first mode, which are adequate for structures whose response is controlled by the fundamental vibration mode. For structures with significant higher mode response, such as plan-asymmetric structures whose three-dimensional seismic response in the inelastic range is very complex, the contribution of all significant modes of vibration should be considered. These kinds of procedures are known as multi-mode pushover analysis (Gupta and Kunnath 2000, Chopra and Goel 2002, Aydinoglu 2003).

There are many recent standards and codes focused on determination of earthquake safety of structures by using displacement-based methods. Some of them are Vision 2000 (1995), ATC 40 (1996), FEMA 273 (1997), FEMA 356 (2000), FEMA 440 (2005), TSDC (2007) and ASCE (2007). Additionally, there have been many studies on displacement-based analysis methods. The Capacity

*Corresponding author, Assistant Professor

E-mail: taner.ucar@deu.edu.tr

^aPh.D.

E-mail: onur.merter@deu.edu.tr

^bProfessor

E-mail: mustafa.duzgun@deu.edu.tr

Spectrum Method compares the capacity of the structure with the demands of earthquake on the structure (Freeman *et al.* 1975, Freeman 1998). The capacity of the structure is represented by a nonlinear force-displacement curve and the demands of the earthquake are represented by response spectra. The intersection of the capacity spectrum and the demand spectrum provides an estimate of the performance of the structure. A relatively simple nonlinear method for the seismic analysis of structures (the N2 method) was developed and the application of the method was illustrated by means of examples (Fajfar and Fischinger 1988, Fajfar and Gaspersic 1996, Fajfar 2000). The N2 method, which has been implemented in EC 8 (2004), combines the pushover analysis of a multi-degree-of-freedom (MDOF) model with the response spectrum analysis of an equivalent single-degree-of-freedom (SDOF) system. Subsequently, the N2 method was extended to asymmetric buildings (Fajfar *et al.* 2005). A statistical study to evaluate the accuracy of proposed approximate methods to estimate the maximum inelastic deformation demand on existing structures was presented by Akkar and Miranda (2005). Goel (2008) evaluated the current nonlinear static procedures specified in FEMA 356 (2000), ASCE (2007), ATC 40 (1996) and FEMA 440 (2005) documents and compared the maximum roof displacement predicted from the nonlinear static procedure with the value derived from earthquake motions. Cao *et al.* (2014) studied the seismic risk assessment of non-seismically designed RC frames by means of damage and fragility analyses.

The use of energy concepts in earthquake resistant structural design has become popular especially in last fifty years. The use of an energy-based earthquake resistant design was first proposed by Housner (1956). Housner (1956) determined the dissipated plastic energy by structures by using the velocity spectra of elastic systems and used the energy concept as a design parameter. Uang and Bertero (1988) made extensive researches on energy-based design parameters and the use of energy as a design criterion in seismic design. Bertero and Gilmore (1994) investigated the use of energy concepts in earthquake resistant analysis and design. Shen and Akbas (1999) investigated the seismic energy demand in steel moment-resisting frames and Akbas *et al.* (2001) developed an energy approach to the performance-based seismic design of steel moment resisting frames. The criteria of performance-based plastic design were discussed and the base shear was calculated by an energy-based design procedure (Lee and Goel 2001). Manfredi (2001) investigated the seismic energy demands of SDOF systems. Leelataviwat *et al.* (2002) proposed a practical design procedure based on conventional plastic design concept with some modifications and used it to design steel moment frames. Akbas and Shen (2003) investigated the energy concept in earthquake resistant design and energy parameters and components of a SDOF system. The hysteresis model, which keeps the complete record of energy dissipation, was developed for deteriorating systems and a damage model was built upon the energy-based low-cycle fatigue concept (Sucuoglu and Erberik 2004). Nonlinear finite element analysis was performed to investigate the cyclic behavioral characteristics of flexure-dominated RC members subject to moderate plastic

displacements (Park and Eom 2006). Leelataviwat *et al.* (2008) proposed a seismic evaluation procedure based on an energy concept and the analysis procedure then was applied to a number of example SDOF and MDOF structural systems to estimate the displacement demands. Eom *et al.* (2009) developed simplified methods for predicting the cyclic force-displacement relationship and energy dissipation of short coupling beams with various reinforcement layouts. As an alternative to current conventional force-based assessment methods, Acun (2010) proposed a performance evaluation procedure for RC columns by using an energy-based approach combined with the low cycle fatigue concept. Acun and Sucuoglu (2012) investigated the energy dissipation capacity of RC columns under cyclic displacements. Liao and Goel (2012) applied the Performance-Based Plastic Design (PBSD) approach to seismic resistant RC special moment frames and seismic demands were estimated by using the work-energy equation. Terapathana (2012) presented a design procedure for RC frames that includes energy demand and nonlinear dynamic time history analyses were conducted in order to estimate the hysteretic energy demand over the height of the building. As an alternative to strength and displacement-based methods, Habibi *et al.* (2013) proposed a stepwise multi-mode energy-based design method for seismic retrofitting with passive energy dissipation systems. The energy-dissipation ability of reinforced concrete frames retrofitted with eccentric buckling-restrained braces was investigated by Yang *et al.* (2017).

In the presented study, plastic energy equations are developed and plastic energy capacities of RC frame structures under monotonic loading are determined graphically by utilizing the developed equations. Nonlinear static analyses are conducted to create energy capacity graphs of five and ten story frames. Seven recorded earthquake time histories, which are frequency-domain scaled and design spectrum compatible, are used in nonlinear time history analyses and the maximum earthquake plastic energy demands are determined. The plastic energy capacities of the frames are examined whether these capacities can resist the plastic energy demands for selected earthquakes or not. An energy-based assessment of the earthquake safety of RC frame structures is carried out by using the plastic energy capacity graphs and earthquake plastic energy demands.

2. Determination of plastic energy dissipated by RC sections

In structural engineering, the energy dissipation of structures under external loads can be explained by a ductile inelastic behavior. The total energy dissipated by a ductile structure is composed of elastic and plastic energy. The elastic energy, which constitutes the very small part of total energy, occurs when the structure behaves linearly elastic and it goes back when the load is removed. Beyond the elastic limit, a ductile structure may undergo large displacements due to small increments in load and in this case a large amount of energy, which is called plastic energy, occurs due to permanent deformations. Elastic energy (E_e) and plastic energy (E_p) regions of an elastic-

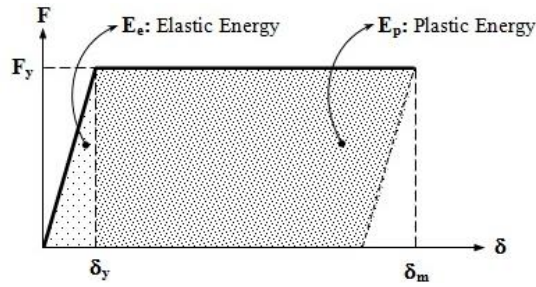


Fig. 1 Elastic and plastic energy in an elastic-perfectly plastic system

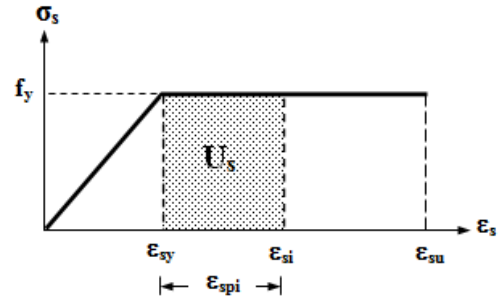


Fig. 2 Stress-strain relation of reinforcement steel

perfectly plastic system are shown in Fig. 1, where F_y is the yield strength, δ_y is the yielding displacement and δ_m is the maximum displacement.

The energy dissipated by plastic hinge regions is required in order to determine the plastic energy dissipation of structures. Simplified equations were developed to evaluate the energy dissipation of RC sections subjected to cyclic loading (Park and Eom 2006, Eom and Park 2010). In this study, the determination of the plastic energy dissipated by RC sections under monotonic loading is based on material strains. The contributions of concrete and reinforcement steel to the plastic energy dissipated by RC sections can be considered individually by using the developed equations. The assumptions of the proposed approach, which is directly based on material strains, are as below.

- Sections are subjected to a monotonic loading.
- A linear strain diagram is taken into consideration due to Navier-Bernoulli Hypothesis.
- Plastic deformations are assumed to be lumped at plastic hinges.
- The plastic energy dissipation of the section is assumed to be equivalent through the plastic hinge length.
- An elastic-perfectly plastic stress-strain relation is considered for reinforcement steel.
- The stress-strain relation, proposed by Mander *et al.* (1988), is implemented for concrete.
- The contribution of concrete to the plastic energy dissipated by RC sections is determined as the sum of the contributions of unconfined and confined concrete.
- The contribution of transverse reinforcement to the plastic energy dissipated by RC sections is indirectly considered by adopting a confined concrete model.
- The contribution of shear strains is neglected.

2.1 Plastic energy equations

The total plastic energy dissipated by RC sections under monotonic loading may be obtained as the sum of contributions of concrete and reinforcement steel to energy. The contribution of reinforcement steel to plastic energy contribution is determined with reference to energy dissipation in unit length and volume of reinforcement steel. The assumed elastic-perfectly plastic stress-strain relation (σ_s - ϵ_s) of reinforcement steel is shown in Fig. 2, where f_y and ϵ_{sy} are the yield stress and strain of reinforcement steel, respectively, ϵ_{si} is the inelastic strain of i^{th} level reinforcement steel, ϵ_{spi} is the plastic strain of i^{th} level reinforcement steel and ϵ_{su} is the ultimate strain. The plastic

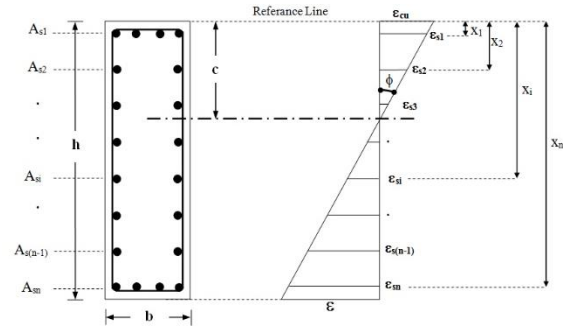


Fig. 3 A typical RC section and strain diagram

energy dissipated by the unit volume of reinforcement steel may be estimated by using the stress-strain relation graph of material.

The plastic energy (U_s) dissipated by the unit volume of reinforcement steel beyond the elastic limit can be expressed as

$$U_s = \sum_{i=1}^n \epsilon_{si} f_y - n \epsilon_{sy} f_y = \sum_{i=1}^n \epsilon_{spi} f_y \quad (1)$$

where n is the total number of reinforcement steel levels. The plastic energy (e_s) dissipated by the unit length of reinforcement steel can be obtained as a result of the integration of plastic energy dissipated by the unit volume over the section area.

$$e_s = \int_A U_s dA = \int_A \left(\sum_{i=1}^n \epsilon_{si} - n \epsilon_{sy} \right) f_y dA = \int_A \left(\sum_{i=1}^n \epsilon_{spi} \right) f_y dA \quad (2)$$

Writing strains of reinforcement steel in terms of curvature and expressing Eq. (2) in absolute value yields the general equation of plastic energy dissipated by the unit length of reinforcement steel.

$$e_s = \sum_{i=1}^n (|c - x_i| A_{si}) \phi f_y - \epsilon_{sy} f_y \left(\sum_{i=1}^n A_{si} \right) \quad (3)$$

In Eq. (3), A_{si} is the cross-sectional area of i^{th} level reinforcement steel, c is the neutral axis, x_i is the depth of the centroid of i^{th} level reinforcement steel and ϕ is the curvature of the section. These parameters are also shown over an illustrative RC section and its linear strain diagram in Fig. 3, where b and h are section dimensions and ϵ_{cu} is the strain of the top fiber of concrete.

In order to determine the contribution of concrete to the plastic energy dissipated by RC sections, unconfined and confined concrete is divided into sufficient number of

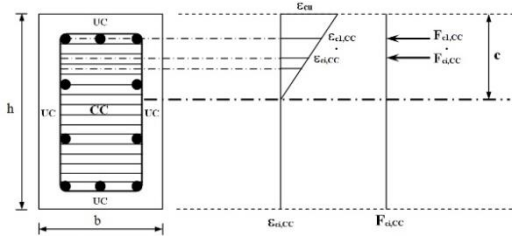


Fig. 4 Resultant strains and compression forces in fibers of confined concrete

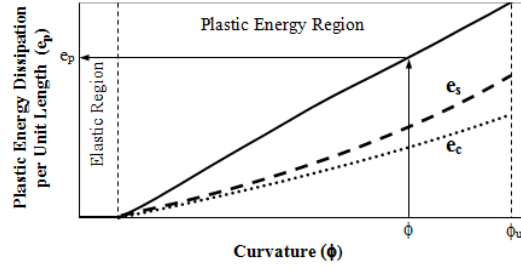


Fig. 5 Plastic energy dissipation-curvature diagram obtained by the proposed approach

fibers. It is obvious that, more accurate results can be obtained by increasing the number of fibers. The contributions of unconfined and confined concrete to the plastic energy dissipation are determined by considering the contribution of each fiber.

Resultant strains and compression forces in individual fibers of confined concrete are shown in Fig. 4, where UC and CC stand for unconfined and confined concrete, respectively, $\epsilon_{ci,CC}$ is the strain and $F_{ci,CC}$ is the force in i^{th} compression fiber of confined concrete.

The contribution of confined concrete (e_{CC}) to the plastic energy dissipated by RC section can be obtained by Eq. (4).

$$e_{CC} = \sum_{i=1} F_{ci,CC} (\epsilon_{ci,CC} - \epsilon_{ce,CC}) \quad (4)$$

Similarly, the contribution of unconfined concrete (e_{UC}) divided into sufficient numbers of fibers to the plastic energy dissipated by RC section may be taken into consideration by Eq. (5)

$$e_{UC} = \sum_{j=1} F_{cj,UC} (\epsilon_{cj,UC} - \epsilon_{ce,UC}) \quad (5)$$

where $\epsilon_{cj,UC}$ is the strain and $F_{cj,UC}$ is the force in j^{th} compression fiber of unconfined concrete. In Eqs. (4)-(5), $\epsilon_{ce,CC}$ and $\epsilon_{ce,UC}$ are the elastic strain limits of confined and unconfined concrete, respectively. In the study, the elastic limit of concrete corresponds to a stress equal to 40% of compression strength of unconfined concrete (f_{co}) (Neville, 1996).

The contribution of concrete to the plastic energy dissipation of RC section under monotonic loading can be determined by Eq. (6).

$$e_c = \sum_{i=1} F_{ci,CC} (\epsilon_{ci,CC} - \epsilon_{ce,CC}) + \sum_{j=1} F_{cj,UC} (\epsilon_{cj,UC} - \epsilon_{ce,UC}) \quad (6)$$

The total plastic energy dissipation of RC section can be obtained as the sum of individual contributions of concrete and reinforcement steel.

$$e_p = e_s + e_c \quad (7)$$

In Eq. (7), e_p is the total plastic energy dissipated by the unit length of RC section and e_c is the contribution of concrete.

Substituting Eqs. (3)-(6) in Eq. (7) yields the general equation of the total plastic energy dissipated by the unit length of RC section.

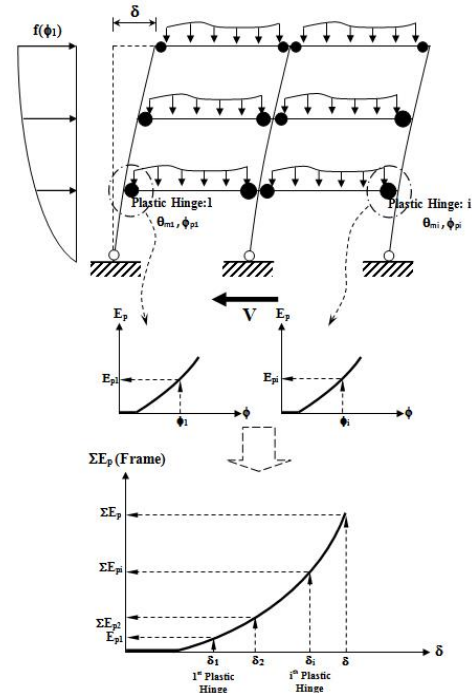


Fig. 6 Plastic energy capacity diagrams of potential plastic hinges and frame

$$e_p = \sum_{i=1}^n (|c - x_i| A_{si}) \phi f_y - \epsilon_{sy} f_y \left(\sum_{i=1}^n A_{si} \right) + \sum_{i=1} F_{ci,CC} (\epsilon_{ci,CC} - \epsilon_{ce,CC}) + \sum_{j=1} F_{cj,UC} (\epsilon_{cj,UC} - \epsilon_{ce,UC}) \quad (8)$$

The total plastic energy dissipated by the plastic hinge (E_p) can be obtain as

$$E_p = e_p \cdot l_p \quad (9)$$

where l_p is the plastic hinge length.

An illustrative plastic energy dissipation-curvature graph, which is obtained by the developed approach, is given in Fig. 5, where contributions of concrete (e_c) and reinforcement steel (e_s) to plastic energy consumption are also shown. Although the area of inelastic part of bending moment-curvature relation graph gives the plastic energy dissipated by the unit length of RC section, the individual contributions of materials to total plastic energy cannot be estimated. The developed approach, which is directly based on material strains, supplies individual contributions of

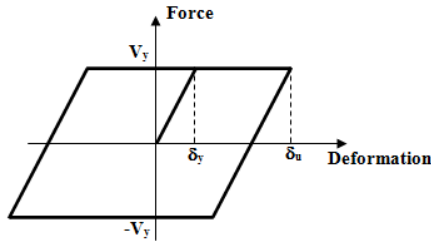


Fig. 7 Cyclic deformation-strength model assumed in dynamic analyses

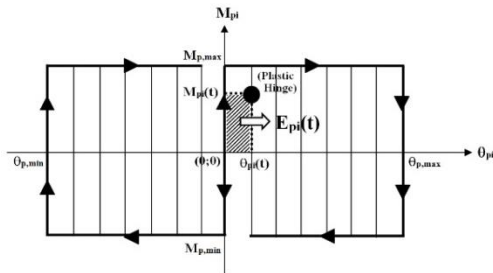


Fig. 8 Cyclic moment-rotation relation and plastic energy dissipation of plastic hinges

concrete and reinforcement steel to the total plastic energy dissipated by RC section.

3. Determination of plastic energy dissipation capacities of RC frames

In this study, the earthquake safety of RC frame structures is evaluated by using plastic energy dissipation capacity graphs of structures obtained by using the proposed approach. Pushover analyses are performed until structural collapse detected and plastic sections are determined. The plastic energy dissipated through the plastic hinge lengths of RC beam and column sections under monotonic loading is obtained by the proposed approach and plastic energy versus curvature relations of plastic sections are determined graphically. Plastic energy dissipation capacities of plastic hinges formed at incremental steps of nonlinear static analysis are determined and the total plastic energy dissipated by the RC frame is obtained as the sum of the plastic energy dissipated by plastic hinges.

The total plastic energy dissipation versus lateral displacement of the top point of the structures is sketched and it is referred to as plastic energy capacity diagram of the structure. The horizontal axis of this diagram is roof displacement and the vertical axis is the total plastic energy dissipated by the structure. An illustrative derivation of the plastic energy capacity diagram is shown in Fig. 6, where potential plastic hinges and plastic energy versus curvature relations of some plastic hinges are also represented.

4. Determination of earthquake plastic energy demand

In the proposed approach for determination of

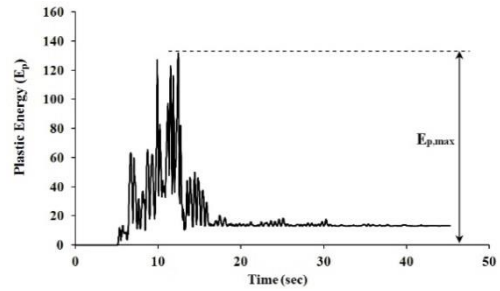


Fig. 9 An illustrative plastic energy-time diagram obtained from dynamic analysis

earthquake safety of RC frame structures, plastic energy dissipation capacities of structures and the maximum plastic energy demand of the selected earthquake records are determined and capacity-demand relation is evaluated in terms of plastic energy. Earthquake plastic energy demands are determined from nonlinear time history analyses by using seven earthquake records. An elastic-perfectly plastic hysteretic model shown in Fig. 7 is considered in nonlinear time history analyses. It should be noted that different results may be obtained by using different hysteretic curves (Clough 1966, Takeda *et al.* 1970). The total plastic energy for each time step of the earthquake record is obtained by using cyclic moment-rotation relations of formed plastic hinges and axial plastic deformations in columns. The total plastic energy dissipated by the structure for each time step of the earthquake is obtained graphically and the maximum plastic energy demand of the earthquake is determined from this graph.

The cyclic moment-rotation relation of a plastic hinge formed in a structural member under earthquake loading can be obtained by using the inelastic part of the assumed hysteretic model. The resultant cyclic moment-rotation curve is shown in Fig. 8, where $M_{p,max}$ and $M_{p,min}$ are plastic moments and $\theta_{p,max}$ and $\theta_{p,min}$ are plastic rotations. $M_{pi}(t)$ is plastic moment, $\theta_{pi}(t)$ is plastic rotation and $E_{pi}(t)$ is plastic energy dissipation of i^{th} plastic hinge at time step t .

The total plastic energy dissipated by the RC structure under an earthquake loading can be obtained as

$$\sum E_{pi}(t) = \sum_{i=1}^{i=n} \left(\sum_{t=0}^{t=\Delta t(m-1)} |M_{pi}(t) \cdot \theta_{pi}(t)| \right) + \sum_{i=1}^{i=n} \left(\sum_{t=0}^{t=\Delta t(m-1)} |N_{pi}(t) \cdot \delta_{pi}(t)| \right) \quad (10)$$

where n is the total number of plastic hinges formed at time step t , m is the total number of the recorded accelerations of the earthquake, Δt is the time interval of accelerations, δ_p is the axial plastic deformation and N_p is the axial plastic load of a column member. The second term of Eq. (10) corresponds to the contribution of axial plastic deformations of columns to the total plastic energy dissipated by the RC structure.

In this study, the maximum earthquake plastic energy demands are determined from the plastic energy dissipation versus time graphs, where the horizontal axis represents the

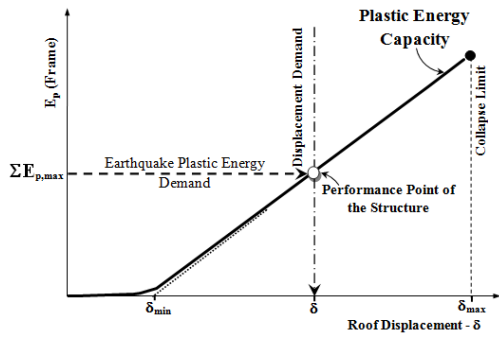


Fig. 10 Plastic energy capacity and earthquake plastic energy demand

Table 1 Design parameters of RC frame structures

	RCF-5.1	RCF-5.5	RCF-10.3	RCF-10.5
G-beam (kN/m)	34.50	35.40	27.05	37.80
Q-beam (kN/m)	14.00	14.00	7.00	14.00
P_G -column (kN)	133.00	135.20 (exterior) 176.80 (interior)	67.60 (exterior) 88.40 (interior)	142.90 (exterior) 188.90 (interior)
P_Q -column (kN)	35.00	35.00 (exterior) 70.00 (interior)	17.50 (exterior) 35.00 (interior)	35.00 (exterior) 70.00 (interior)
T_1 -uncracked (sec)	0.67	0.64	0.97	1.05
BEAMS (cm×cm)	30×60	30×60	30×60	30×70
COLUMNS (cm×cm)	50×50 (@Story: 1-2&3)	55×55 (@Story: 1-2&3)	60×60 (@Story: 1-2-3&4) 55×55 (@Story: 5-6&7)	60×60 (@Story: 1-6) 55×55 (@Story: 7-10)

duration of an earthquake. The plastic energy values for each time step of the earthquake are obtained as a result of converting cyclic moment-plastic rotations of plastic hinges to monotonic loading. A typical earthquake plastic energy demand-time graph is shown in Fig. 9, where $E_{p,max}$ is the maximum value of earthquake plastic energy demand. The maximum value of earthquake plastic energy demand may be obtained at any time of earthquake duration. The instant variations in plastic energy-time graphs are due to cyclic behavior of plastic hinges.

5. Energy-based determination of earthquake safety of RC structures

In this study, the determination of earthquake safety of RC frame structures is based on the comparison of plastic energy dissipation capacities of structures with the maximum earthquake plastic energies. The plastic energy dissipation capacities of the RC frame structures under monotonic loading are examined whether these capacities can resist the plastic energy demands for selected earthquakes or not. The safety of the RC frame structures under earthquake effects is researched by using an energy-based assessment approach.

The plastic energy dissipation capacity of the structure under monotonic loading and the earthquake plastic energy demand is shown in Fig. 10. The plastic energy dissipation capacity graphs are obtained by the proposed approach. The intersection point of the earthquake plastic energy demand level with the plastic energy dissipation capacity gives the

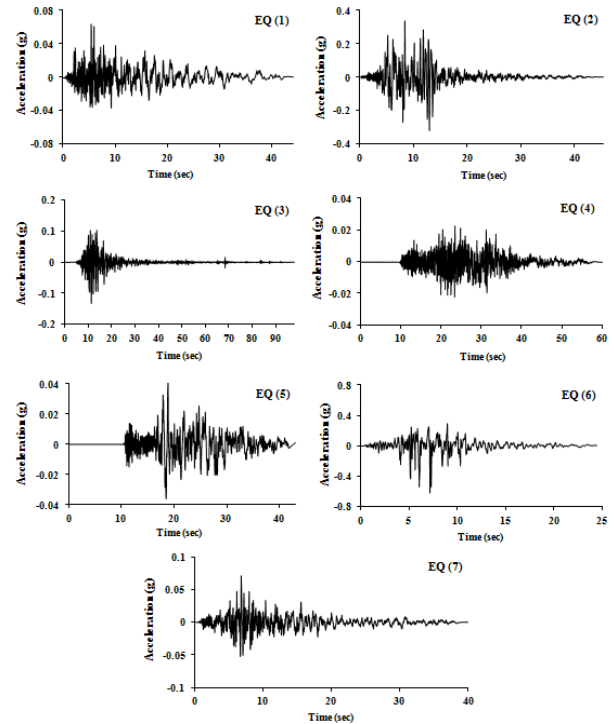


Fig. 11 Acceleration time histories of earthquakes

energy-based performance point. The displacement component of energy-based performance point corresponds to the target displacement of the structure, which can also be determined by different methods.

The plastic energy dissipation capacity of the structure and the earthquake plastic energy demand are the two necessary parameters of energy-based assessment of earthquake safety of structures. The structure cannot withstand the earthquake in case the earthquake plastic energy demand exceeds the expected plastic energy dissipation capacity of the structure. If the structure has plastic energy capacity over the plastic energy demand of the earthquake, it means that the earthquake safety of the structure is ensured.

6. Case study

The proposed energy-based approach is applied to 5- and 10-story regular RC two-dimensional frame structures and the earthquake safety of these structures is assessed. Material properties are assumed to be 25 MPa for the concrete compressive strength and 420 MPa for the yield strength of both longitudinal and transverse reinforcements. 5-story one- and five-bay RC frame structures (RCF-5.1 and RCF-5.5) and 10-story three- and five-bay RC frame structures (RCF-10.3 and RCF-10.5) are designed in accordance with the TSDC (2007). It is a common approach to analyze two-dimensional frames instead of using three-dimensional structures having regular distribution of stiffness and mass (ElAssaly 2013). Frame structures are assumed to be on the Seismic Zone 1 and the Local Site Class is taken as Z3. Typical story heights are 3 meters and spans are 5 meters. There exist uniformly distributed dead

Table 2 Details of ground motion records

EQ. No.	Earthquake & Date	M_w	R_{JB} (km)	V_{S30} (m/s)	PGA (g)	PGV (cm/s)	PGD (cm)
1	Parkfield, 28.06.1966	6.19	17.64	408.9	0.063	6.8	3.55
2	Hector Mine, 16.10.1999	7.13	10.35	684.9	0.3062	34.21	17.71
3	Chi-Chi, Taiwan-04, 20.09.1999	6.2	12.40	680	0.1226	15.86	5.64
4	Duzce (Sakarya St.), 12.11.1999	7.14	45.20	471	0.023	5.5	7.34
5	Duzce (Lamont St.), 12.11.1999	7.14	23.40	517	0.042	9.2	8.07
6	Victoria, Mexico, 06.09.1980	6.33	13.80	659.6	0.621	31.6	13.2
7	Chalfant-Valley, 21.07.1986	6.19	29.40	338.5	0.0635	3.79	1.26

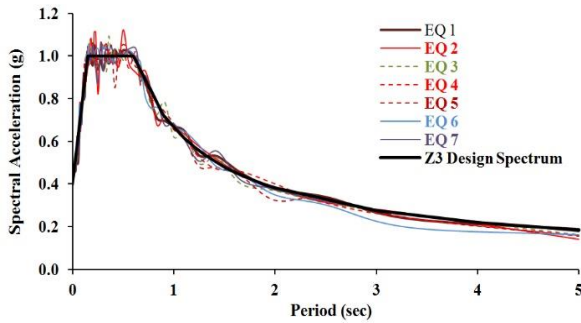


Fig. 12 Scaled acceleration spectra of earthquakes and the design spectrum

(G) and live (Q) loads in all spans and concentrated dead (P_G) and live (P_Q) loads in columns. The values of the considered loads, the dimensions of beams and columns and the values of the fundamental vibration period are given in Table 1. There exists twelve symmetrically distributed longitudinal bars in all columns and the diameter of these bars is between 18-24 mm. Longitudinal bars with diameter 16 mm and 18 mm are used for beams. The diameter of transverse reinforcement is 10 mm and the spacing of transverse reinforcement is calculated by considering the requirements of confinement and central zones defined in TSDC (2007).

Nonlinear dynamic analyses of frames are performed by using the time histories of recorded earthquakes. The accelerograms for the earthquakes are constructed by using the data provided from the official web site of the Pacific Earthquake Engineering Research Center (PEER 2015). Details of the ground motion records are given in Table 2, where M_w is the moment magnitude of earthquake, R_{JB} is the Joyner-Boore distance, V_{S30} is the average of shear wave velocity in the first 30 m of the soil, PGA is the peak ground acceleration, PGV is the peak ground velocity and PGD is the peak ground displacement. The selected ground motions have strike-slip fault mechanism and satisfy all the conditions given in TSDC (2007). The effects of near fault are not considered in the selected earthquake records. Acceleration time histories of the earthquakes are shown in Fig. 11.

The frequency-domain scaled and design spectrum compatible acceleration spectra of the selected ground motions are shown together with the design spectrum of TSDC (2007) for local site class Z3 in Fig. 12.

Nonlinear time history analyses are performed by using the structural analysis program SAP2000 v.15.1.0

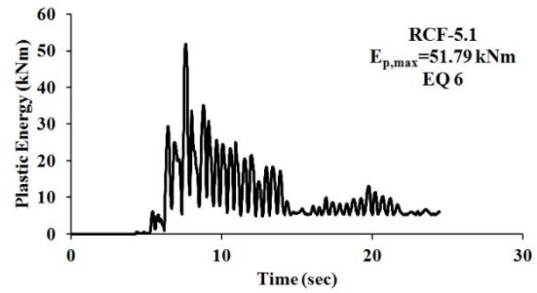


Fig. 13 Plastic energy-time diagram of RCF-5.1 for EQ 6

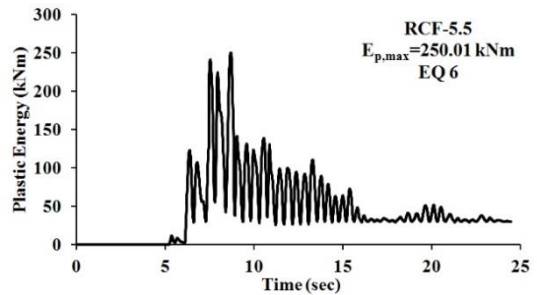


Fig. 14 Plastic energy-time diagram of RCF-5.5 for EQ 6

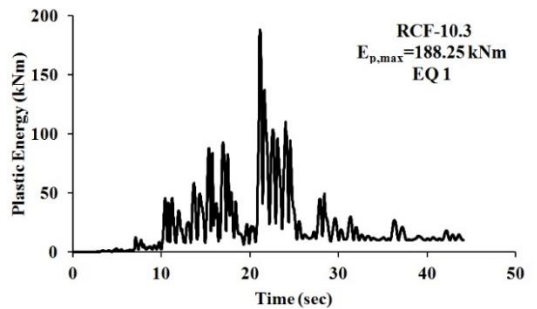


Fig. 15 Plastic energy-time diagram of RCF-10.3 for EQ 1

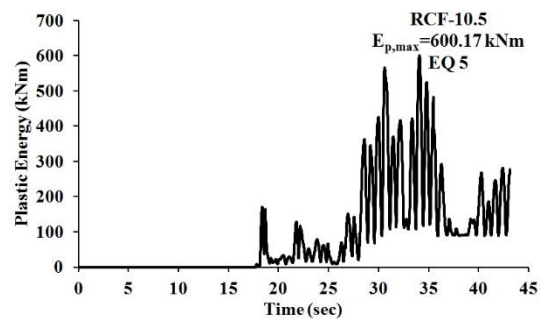


Fig. 16 Plastic energy-time diagram of RCF-10.5 for EQ 5

(Computers and Structures Inc 2011). As a result, earthquake plastic energy demands are determined and they are used for energy-based earthquake safety assessment of the RC frames.

6.1 Determination of the maximum earthquake plastic energy demand of RC frames

Plastic energy dissipation versus time graphs are obtained as a result of nonlinear time history analyses of considered multi-story RC frame structures. The maximum plastic energy demands are determined by using these

plastic energy graphs. Plastic energy values are determined as it is obtained from Eq. (10).

The maximum earthquake plastic energy demand values of the frames RCF-5.1 and RCF-5.5 are determined from the plastic energy dissipation versus time graphs of the earthquake 6 (EQ 6). For five-story RC frames, EQ 6 gives the maximum values of plastic energy demand among the selected earthquakes. The plastic energy dissipation versus time graphs of the frames RCF-5.1 and RCF-5.5 under the effect of EQ 6 are shown in Figs. 13-14.

In Fig. 15, the maximum earthquake plastic energy demand of RCF-10.3 is determined by using the plastic energy graph of EQ 1. The maximum earthquake plastic energy demand of RCF-10.5 is obtained from the plastic energy graph of EQ 5 (Fig. 16). Plastic energy versus time graphs which are obtained from nonlinear time history analyses within the study depend on cyclic moment-rotation relations of plastic hinges and axial plastic deformations of column members. Therefore, plastic energy graphs and the maximum plastic energy demand values obtained from these graphs depend directly on the acceptances of nonlinear time history analyses.

6.2 Energy-based assessment of earthquake safety of RC frames

Single-mode nonlinear static pushover analysis up to the collapse is performed for the frame structures. The plastic energy dissipations of plastic hinge regions of the frames under monotonic loading are calculated by using the presented approach. Plastic energy dissipation versus curvature relations are obtained for all plastic hinges in the structures. Then, the total plastic energy of the frame structures under monotonic loading are obtained graphically according to roof displacements. The obtained energy graphs are referred as the “plastic energy capacity graphs”. The plastic energy capacity graphs of RC structures are used to investigate the earthquake safety of the structures.

Nonlinear static pushover analyses are performed by using SAP2000 v.15.1.0 software. Plastic hinge hypothesis is used to define nonlinear behavior of the material in nonlinear analyses. Geometrical variations are taken into account in equilibrium equations. Moment versus plastic rotation ($M-\theta_p$) relation of structural members is obtained by using the program which is developed in Excel software. Moment versus plastic rotation graphs are idealized by the rigid-plastic behavior. Rigidities of cracked beam and column sections are taken into account in nonlinear analyses as indicated in the TSDC (2007). It is accepted that shear capacity limits of structural members are not exceeded.

In Figs. 17-20, the maximum plastic energy demand levels of frame structures which are obtained by using nonlinear time history analyses are shown by straight lines. In these graphs, the mean plastic energy demand of earthquakes is indicated by red straight lines. Plastic energy values which are greater and less than the mean plastic energy demands in the amount of standard deviation are indicated as red dotted lines in the plastic energy capacity graphs. Plastic energy levels shown by straight lines in the plastic energy capacity graphs are the levels that show the

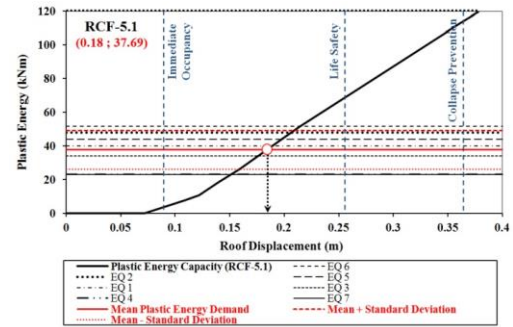


Fig. 17 Plastic energy capacity of RCF-5.1 and maximum earthquake plastic energy demands

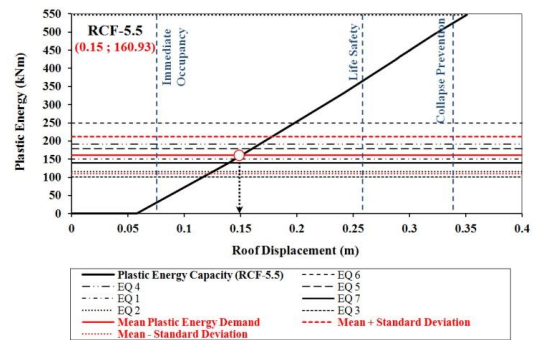


Fig. 18 Plastic energy capacity of RCF-5.5 and maximum earthquake plastic energy demands

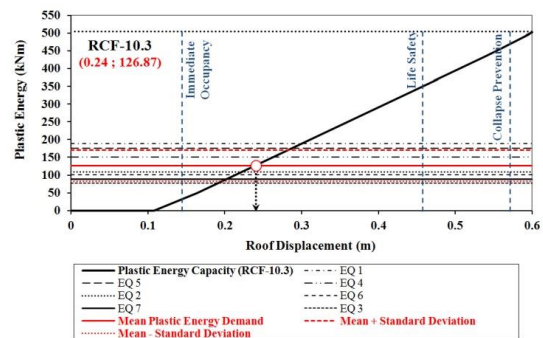


Fig. 19 Plastic energy capacity of RCF-10.3 and maximum earthquake plastic energy demands

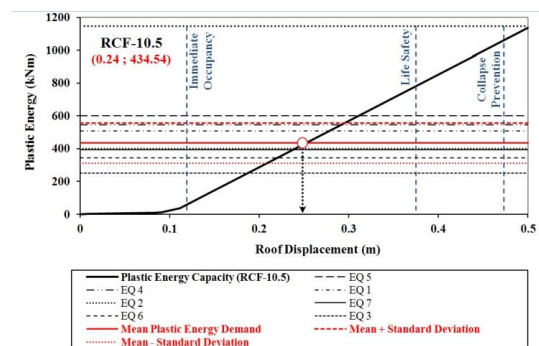


Fig. 20 Plastic energy capacity of RCF-10.5 and maximum earthquake plastic energy demands

maximum values of different earthquake plastic energy demands. Structural performance levels, which take place in the plastic energy capacity graphs, are determined by using

Table 3 Code-based and energy-based displacement demand of frames

Frame	Target displacement (cm)			Displacement corresponds to the mean earthquake plastic energy demand (cm)
	FEMA 440	ASCE 41-06	TSDC	
RCF-5.1	20.90	22.30	20.67	18.39
RCF-5.5	18.40	19.67	18.83	14.92
RCF-10.3	31.09	31.10	32.65	23.96
RCF-10.5	32.07	32.10	34.49	24.19

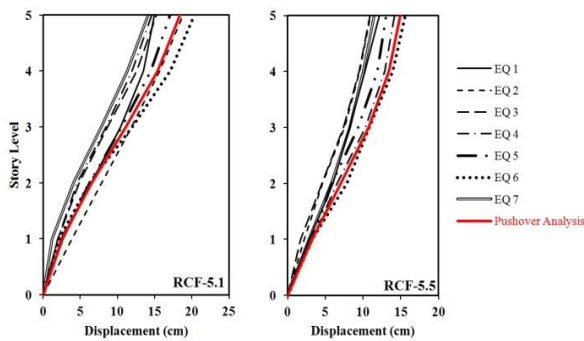


Fig. 21 Lateral displacements of 5 story frames

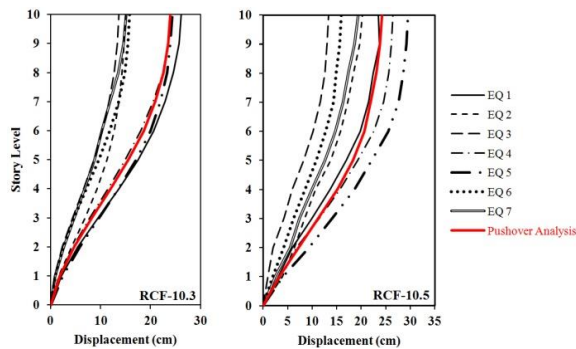


Fig. 22 Lateral displacements of 10 story frames

the conditions of TSDC (2007). Upper limits of the strain values of steel reinforcement and compression strain of the top fiber of concrete are taken into account as indicated in the TSDC (2007).

The intersections of the mean plastic energy demands with the plastic energy capacity graphs represent performance points of the selected frame type structures. In the graphs, the coordinates of the obtained performance points of the five and ten-story frames are given in terms of displacement and plastic energy.

Energy analyses consist of displacement concept with the same time. Plastic energy target (plastic energy demand/energy-based performance point/total plastic energy dissipation) of the structure occurs in the definite displacement value. Because of this, earthquake plastic energy demands of the frames obtained within the study correspond to the certain target displacement value. In other words, the earthquake plastic energy demand level gives the displacement demand of the structure by itself. In Table 3, the displacements that correspond to the mean earthquake plastic energy demands are given with the code-based displacement demand values. The displacement demands

obtained from different procedures are not definitely the same. Similar results are found by Hakim *et al.* (2014). However, these displacement values are close to each other. Also, the displacement demand values obtained by the proposed approach are found to be consistent with the code-based results. In Figs. 21-22, displacements of story tops of the structures obtained from nonlinear time history analyses with selected earthquake records and nonlinear pushover analyses at the performance points are given.

7. Conclusions

An energy-based approach for evaluation of earthquake safety of multi-story RC frame structures is presented in the study. The approach is based on comparison between earthquake plastic energy demands and plastic energy capacities of RC frame structures under monotonic loading. Plastic energy capacity limits of the five and ten-story frame structures are not exceeded under selected earthquake records. Plastic energy capacities of the multi-story RC structures in monotonic nonlinear behavior satisfy the plastic energy demands of the selected earthquakes. Summary of important findings and innovations from the energy-based structural evaluation approach used in this study can be written as the following:

- It is observed that the steel reinforcement contributes most to the plastic energy dissipation of flexural RC members under monotonic loading.
- With increasing axial load in combined bending and axially compression loaded RC members, strain values become important in the members and concrete material contribute to the plastic energy dissipation together with the ductile steel reinforcement material.
- Contribution of concrete material to the plastic energy dissipation in combined bending and axially loaded members increases to a certain degree with increasing axial load level. However, plastic energy dissipation cannot be mentioned when high levels of axial load acts to the section. In this case, section does not behave ductile and plastic energy concept is not defined.
- In classical nonlinear static pushover analysis methods, displacements and plastic energies are calculated for only roof level of the structure. However, plastic energy dissipations of all stories in the frame type structures can be calculated by using the energy-based evaluation approach within the study.
- Because of using energy-based analyses, the existing approach in the study may be applied to the frame structures which do not use rigid diaphragm assumption in structural design.
- Plastic energies of frame structures in nonlinear behavior are obtained by using a new approach which is based on material strains.
- The earthquake plastic energy demand is determined graphically in the view of specified acceptances. The maximum plastic energy demands are obtained from plastic energy versus time graphs and used in evaluation of earthquake safety of mid-rise frame type structures.
- Structural performance levels which are described in the force-displacement curves in performance-based seismic design codes are defined in the plastic energy capacity graphs.

- Structural performance points are determined by using energy-based approach and obtained in the form of target plastic energy (earthquake mean plastic energy demand) and target displacement.

- It is observed that the displacement results obtained from nonlinear static pushover analyses until the plastic energy demands are reached are close to the results of nonlinear time history analyses.

- The displacements correspond to the mean plastic energy demands are obtained quite close to the displacements determined by using different seismic design codes.

The acceptances in nonlinear analyses play a very important role in validity of the analysis results. Modelling of plastic hinge regions in nonlinear analyses is important from the point of precision modelling of plastic energy capacity graphs. Because of this, acceptances considered in the analyses should be understood while evaluating the results. Researches should be developed for usability of the existing energy-based approach on different type of structural systems.

References

- Acun, B. (2010), "Energy based seismic performance assessment of reinforced concrete columns", Ph.D. Dissertation, Middle East Technical University, Ankara, Turkey.
- Acun, B. and Sucuoğlu, H. (2012), "Energy dissipation capacity of reinforced concrete columns under cyclic displacements", *ACI Struct. J.*, **109**(4), 531-540.
- Akbas, B. and Shen, J. (2003), "Earthquake resistant design and energy concepts", *Tech. J.-Digest*, **14**(2), 865-888.
- Akbas, B., Shen, J. and Hao, A.H. (2001), "Energy approach in performance-based seismic design of steel moment resisting frames for basic safety objective", *Struct. Des. Tall Build.*, **10**(3), 193-217.
- Akkar, S.D. and Miranda, E. (2005), "Statistical evaluation of approximate methods for estimating maximum deformation demands on existing structures", *J. Struct. Eng.*, **131**(1), 160-172.
- ASCE (2007), *ASCE/SEI 41-06: Seismic Rehabilitation of Existing Buildings*, American Society of Civil Engineers, Reston, Virginia, U.S.A.
- ATC 40 (1996), *Seismic Evaluation and Retrofit of Concrete Buildings*, Applied Technology Council, Washington, U.S.A.
- Aydinoğlu, M.N. (2003), "An incremental response spectrum analysis procedure based on inelastic spectral displacements for multi-mode seismic performance evaluation", *Bull. Earthq. Eng.*, **1**(1), 3-36.
- Bertero, V.V. and Gilmore, A.T. (1994), *Use of Energy Concepts in Earthquake Resistant Analysis and Design: Issues and Future Directions*, Advances in Earthquake Engineering Practice, Short Course in Structural Engineering, Architectural and Economic Issues, University of California, Berkeley, U.S.A.
- Cao, V.V., Ronagh, H.R. and Baji, H. (2014), "Seismic risk assessment of deficient reinforced concrete frames in near-fault regions", *Adv. Concrete Constr.*, **2**(4), 261-280.
- Chopra, A.K. and Goel, R.K. (2002), "A modal pushover analysis procedure for estimating seismic demands for buildings", *Earthq. Eng. Struct. Dyn.*, **31**(3), 561-582.
- Clough, R.W. (1996), *Effects of Stiffness Degradation on Earthquake Ductility Requirement*, University of California, Berkeley, U.S.A.
- Computers and Structures Inc (2011), *SAP2000: Integrated Structural Analysis and Design Software*, CSI, Version 15.1.0, Berkeley, U.S.A.
- EC 8 (2004), *Eurocode 8: Design of Structures for Earthquake Resistance-Part 1: General Rules, Seismic Actions and Rules for Buildings*, European Committee for Standardization, Brussels, Belgium.
- ElAssaly, M. (2013), "Towards seismic vulnerability assessment of the building stock in Egypt", *Arab. J. Sci. Eng.*, **38**(11), 2953-2969.
- Eom, T.S. and Park, H.G. (2010), "Evaluation of energy dissipation of slender reinforced concrete members and its applications", *Eng. Struct.*, **32**(9), 2884-2893.
- Eom, T.S., Park, H.G. and Kang, S.M. (2009), "Energy based cyclic force displacement relationship for reinforced concrete short coupling beams", *Eng. Struct.*, **31**(9), 2020-2031.
- Fajfar, P. (2000), "A nonlinear analysis method for performance-based seismic design", *Earthq. Spec.*, **16**(3), 573-592.
- Fajfar, P. and Fischinger, M. (1988), "N2-A method for non-linear seismic analysis of regular buildings", *Proceedings of the 9th World Conference on Earthquake Engineering*, Tokyo, Kyoto, Japan, August.
- Fajfar, P. and Gaspersic, P. (1996), "The N2 method for seismic damage analysis of RC buildings", *Earthq. Eng. Struct. Dyn.*, **25**(1), 31-46.
- Fajfar, P., Marusic, D. and Perus, I. (2005), "Torsional effects in the pushover-based seismic analysis of buildings", *J. Earthq. Eng.*, **9**(6), 831-854.
- FEMA 273 (1997), *NEHRP Guidelines for the Seismic Rehabilitation of Buildings*, Federal Emergency Management Agency, Washington, U.S.A.
- FEMA 356 (2000), *Prestandard and Commentary for the Seismic Rehabilitation of Buildings*, Federal Emergency Management Agency, Washington, U.S.A.
- FEMA 440 (2005), *Improvement of Nonlinear Static Seismic Analysis Procedures*, Federal Emergency Management Agency, Washington, U.S.A.
- Freeman, S.A. (1998), "Development and use of capacity spectrum method", *Proceedings of the 6th U.S. National Conference on Earthquake Engineering*, Seattle, Washington, U.S.A., May.
- Freeman, S.A., Nicoletti, J.P. and Tyrell, J.V. (1975), "Evaluations of existing buildings for seismic risk-a case study of puget sound naval shipyard, Bremerton, Washington", *Proceedings of the U.S. National Conference on Earthquake Engineering*, Ann Arbor, Michigan, U.S.A., June.
- Goel, R.K. (2008), "Evaluation of current nonlinear static procedures for reinforced concrete buildings", *Proceedings of the 14th World Conference on Earthquake Engineering*, Beijing, China, October.
- Gupta, B. and Kunnath, S.K. (2000), "Adaptive spectra-based pushover procedure for seismic evaluation of structures", *Earthq. Spec.*, **16**(2), 367-391.
- Habibi, A., Chan, W.K. and Albermani, F. (2013), "Energy-based design method for seismic retrofitting with passive energy dissipation systems", *Eng. Struct.*, **46**, 77-86.
- Hakim, R.A., Alama, M.S. and Ashour, S.A. (2014), "Seismic assessment of RC building according to ATC 40, FEMA 356 and FEMA 440", *Arab. J. Sci. Eng.*, **39**(11), 7691-7699.
- Housner, G.W. (1956), "Limit design of structures to resist earthquakes", *Proceedings of the 1st World Conference on Earthquake Engineering*, Berkeley, California, U.S.A., June.
- Lee, S.S. and Goel, S.C. (2001), *Performance Based Design of Steel Moment Frames Using Target Drift and Yield Mechanism*, Research Report UMCEE 01-17, Department of Civil and Environmental Engineering, University of Michigan, U.S.A.
- Leelataviwat, S., Goel, S.C. and Stojadinovic, B. (2002), "Energy based seismic design of structures using yield mechanism and

- target drift”, *J. Struct. Eng.*, **128**(8), 1046-1054.
- Leelataviwat, S., Saewon, W. and Goel, S.C. (2008), “An energy based method for seismic evaluation of structures”, *Proceedings of the 14th World Conference on Earthquake Engineering*, Beijing, China, October.
- Liao, W.C. and Ve Goel, S.C. (2012), “Performance-based plastic design and energy based evaluation of seismic resistant RC moment frame”, *J. Mar. Sci. Technol.*, **20**(3), 304-310.
- Mander, J.B., Priestley, M.J.N. and Park, R. (1988), “Theoretical stress-strain model for confined concrete”, *J. Struct. Div.*, **114**(8), 1804-1826.
- Manfredi, G. (2001), “Evaluation of seismic energy demand”, *Earthq. Eng. Struct. Dyn.*, **30**(4), 485-499.
- Neville, A. (1996), *Properties of Concrete*, John Wiley & Sons, New York, U.S.A.
- Park, H.G. and Eom, T.S. (2006), “A simplified method for estimating the amount of energy dissipated by flexure dominated reinforced concrete members for moderate cyclic deformations”, *Earthq. Spec.*, **22**(3), 459-490.
- PEER Strong Ground Motion Database (2015), <http://ngawest2.berkeley.edu/>
- Shen, J. and Akbas, B. (1999), “Seismic energy demand in steel moment frames”, *J. Earthq. Eng.*, **3**(4), 519-559.
- Sucuoglu, H. and Erberik, A. (2004), “Energy-based hysteresis and damage models for deteriorating systems”, *Earthq. Eng. Struct. Dyn.*, **33**(1), 69-88.
- Takeda, T., Sozen, M.A. and Nielsen, N.N. (1970), “Reinforced concrete response to simulated earthquakes”, *J. Struct. Div.*, **96**(12), 2557-2573.
- Terapathana, S. (2012), “An energy method for earthquake resistant design of RC structures”, Ph.D. Dissertation, University of Southern California, Los Angeles, U.S.A.
- TSDC (2007), *Turkish Seismic Design Code*, Ministry of Public Works and Settlement, Ankara, Turkey.
- Uang, C.M. and Bertero, V.V. (1988), *Use of Energy as a Design Criterion in Earthquake Resistant Design*, Report No. UCB/EERC-88/18, Earthquake Engineering Research Center, University of California, Berkeley, U.S.A.
- Vision 2000 (1995), *Performance Based Seismic Engineering of Buildings*, Structural Engineers Association of California, Sacramento, California, U.S.A.
- Yang, Y., Liu, R., Xue, Y. and Li, H. (2017), “Experimental study on seismic performance of reinforced concrete frames retrofitted with eccentric buckling-restrained braces (BRBs)”, *Earthq. Struct.*, **12**(1), 79-89.